Hydrologically-based topographic effect on landslide characteristics: the case of the 2018 M_w6.7 Eastern-Iburi earthquake in Hokkaido

Rasis Putra RITONGA[1*], Takashi GOMI[1], Roy C SIDLE[2], Rozaqqa NOVIANDI[1], and Yohei ARATA[1]

[1] United Graduate School of Agricultural Science, Tokyo University of Agriculture and Technology, Japan
[2] Mountain Societies Research Institute, University of Central Asia, Tajikistan

1. INTRODUCTION

Earthquake-induced landslides (EIL) are controlled by the geomorphic characteristics of rather steep and convex topography (Sidle and Ochiai, 2006). For instance, during the 2016 Kumamoto earthquake case in Japan (M_w=7.0), landslides were mostly found on laterally convex hillslopes (65%) and upwardly convex landforms (77%) (Koyanagi et al., 2020). For the 2018 Eastern Iburi earthquake in Japan (M_w=6.7), Ritonga et al., (2021) found that landsides were more susceptible on slope gradient ranges >35°.

Hydrological conditions affect the probability of the occurrence of landslides because those factors can influence the subsurface hydrology in the soils (Sidle et al., 2019). For EIL, Sidle and Ochiai (2006) mentioned high soil moisture could destabilize and liquify the hillslope by also increasing pore water pressures, especially in moist soft soils and unconsolidated deposits. Hence, most studies on hydrological condition and slope stability have focused on rainfall-induced landslides studies rather than EIL.

Local topography strongly influences the soil-hydrological conditions and alters characteristics of landslides. In general, concave hillslopes are more susceptible for landsliding due to increasing of pore water pressures as the result of convergent subsurface flow to the hollow (Tsuboyama et al., 2000). For instance, 70% of landslides were collapsed on the concave-shaped hillslopes due to high rates of infiltration into the center of hollow topography, leading to excess soil moisture and pore water pressures (Dahal et al., 2008). Based on these findings, the role of topographic condition on soil moisture likely affects the probability and mobility of EIL. Hence, interaction among soil moisture condition, topography, and probability of EIL have never been examined, while the importance had been mentioned qualitatively (Wang et al., 2019).

Understanding hydrologically-based topographic conditions on hillslopes is crucial for evaluating new perspectives of zoning hazardous areas in earthquake-induced landslide studies. Therefore, the objectives of this study are: (i) examining the hydrologically-based topography of landslides; and (ii) characterizing the position of landslides and its correlation with hydrologically-based topographic measurements.

2. STUDY AREA AND METHODOLOGY

On 6 September 2018, the Eastern Iburi EIL triggered up to 6117 shallow landslides. These occurred just one day after Typhoon no. 21 Jebi left torrential rains and the affected area also experienced intense rainfall (cumulative rainfall: 230-300 mm) from two weeks before the earthquake. We selected 18.9 km^2 in Tomisato area, Iburi with elevation ranging from 36 to 400 m. The mean annual precipitation and air temperature are 997 mm and 6.7°C, respectively. The surface geology of this area consists of neogene mudstone, sandstone, and conglomerate. Soil depth in this area ranged from 1 to 4 m. Tarumae volcano is the most recent event, which produced pyroclastic deposits in the area including Tarumae b (Ta-b: 1667 A.D.), c (Ta-c: 2.5 ka), and d (Ta-d: 8.7-9.2 ka).

We delineated landslide scars using both LiDAR shaded relief (0.5 m) and orthophoto images (0.2 m). As the availability of high-resolution shaded relief, we were able to detect landslides under dense forest canopies (<20 m^2). Topographic parameters, such as curvature, were also derived using post-earthquake LiDAR-DEM (0.5 m).

To estimate hydrological conditions, Topographic Wetness Index (TWI) derived from a post-earthquake LiDAR-DEM was used. We assumed the topographic profile post-earthquake was similar to the pre-earthquake condition. We adopted the method proposed by (Rozycka et al., 2016), eliminating specific range of TWI cells value because the method can represent possible zones of high soil moisture as the most susceptible hillslope elements. We used the mean TWI value (mean = 3) to obtain the raster cells that only represent "*high soil moisture cells*" **(Fig. 1a, b)**. After assessing the TWI >3 values, raster cell counts (RCC) were extracted in each landslide. RCC then were used to represent *degree of wetness* (Dw) by comparing RCC of TWI >3 values with the total of RCC in one landslide delineation:

$$Degree\ of\ wetness\ (Dw) = \frac{RCC\ (TWI>3)}{total\ RCC\ in\ a\ landslide} \quad [1]$$

To characterize possible spatial soil moisture condition in the landslide-affected area, Dw is classified as three types: (a) *Low wetness (Lw)*, represented by TWI >3 raster cells which contained <30% (Dw<0.3) total raster cells in one landslide; (b) *Moderate wetness (Mw)*, represented Dw 30%-70% (0.3 < Dw<0.7); and (c) *High wetness (Hw)*, represented Dw >70% (Dw>0.7).

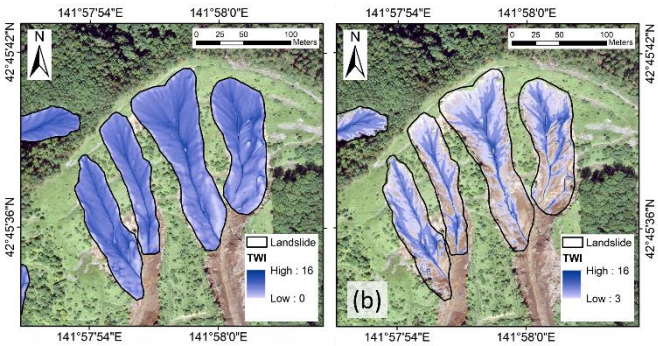

Fig 1. (a) Landslides TWI; (b) Landslides TWI with value >3

The landslide position was calculated based on Meunier et al., (2008), representing the landslide position on the hillslope and as an indicator to assess possible impacts to the channel. The calculation was based on the normalization of the nearest distance of landslides with respect to ridges and streamlines:

$$\left|d_{st,top}\right| = \frac{d_{st,top}}{d_{st}+d_{top}} \quad [2]$$

$|d_{st}|$ has value ranging from 0 for a landslide located in the stream network to 1 for a ridgeline. $|d_{top}|$ also has the same value assessed in the opposite way. $|d_{st} + d_{top}|$ means the total of hillslope length

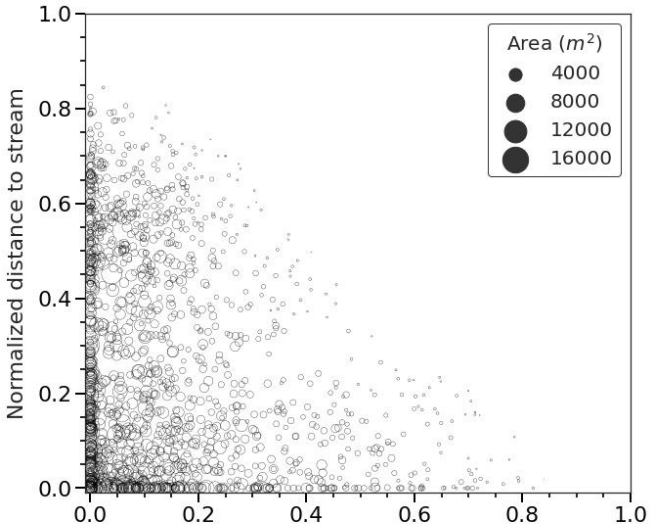

Fig 2. Normalized distance of ridge line and streamline to landslides in respect of area

where landslide occurred. The nearest distance to landslide was analyzed using *Near* tool from ArcMap 10.5.

3. RESULTS

We delineated 1440 landslide scars in the 18.9 km^2 study area. Based on landslide frequency-size distribution, the highest frequency density occurred within 650-1050 m^2 (0.65 m^{-2}). The exponent power law decay (medium-size landslides) was -3.5 (R^2 = 0.98). Based on curvature characteristics, 79% of the landslides were considered concave, 6% convex, and 88% concentrated on planform topography.

We found 56.4% of the landslides were dominantly clustered near stream and ridge (NT_{rs}), followed by near the ridge of upper quart of the slopes (NT_r), and far from the streamline (NT_s) (11.5%) **(Fig. 2)**. The largest landslide area was found near the stream and ridge (mean: 2472 m^2), followed by the near ridge (mean: 793 m^2), and near stream (mean: 246 m^2). This result suggests that the entire slope (upper quarter to lower quarter) was mostly collapsed and thus triggered larger landslides. *Degree of wetness* (*Dw*) for NT_{rs} landslides ranged from 0.07 to 0.85 with a mean of 0.48 (SD: 0.13). The mean *Dw* for NT_r was 0.48 (SD: 0.16), while the mean *Dw* for NT_s was 0.38 (SD: 0.25).

4. DISCUSSION

Among the 1440 landslides, we found 14% of landslides considered as *Lw landslides*, 68% as *Mw*, and 18% as *Hw.* This indicates Iburi landslides mostly tended to collapse with topography that has medium-high soil moisture. We noticed the trend of *Dw* of landslides induced by Iburi earthquake might also show the similar topographic characteristics of rainfall-induced landslides case with the condition of high soil moisture and pore water pressures, particularly on concave curvatures (Dahal et al., 2008). The higher water content found on TWI >3 topography, implies that higher *Dw* cells made the hillslopes more susceptible by increasing the soil moisture and pore water pressures caused by two-weeks of rainfall (Noviandi et al., 2019).

Most of landsides in Iburi affected the entire hillslope from ridge top to streams based on NT_{rs}. We assumed the special case of this landslides cluster was affected by the different *degree of wetness*. This pattern of landslides differed compared to previous EIL studies. EIL tended to cluster on the upper quarter of hillslopes as the seismic amplification is greatest near the ridge crest. For instance, Saito et al., (2018) compared landslides induced by rainfall and earthquakes in Aso Volcano area, Japan and found about 54% landslides clustered near the stream ($ND_r > 0.2$) while earthquake-induced landslides were mostly found near the ridge ($ND_r < 0.2$).

Because higher values of *Dw* in NT_{rs} occurred, high soil moisture condition might destabilize entire hillslopes starting from ridge initiation (as the seismic amplification was high) (Meunier et al., 2008), then affecting the rest of the lower susceptible part causing a collapse on concave topography that could accumulate and trigger higher levels of pore water pressure. This result was similar to Marc et al., (2018) who noted the greater size of worldwide rainfall-induced landslides was strongly affected by higher soil moisture and pore water pressures as the result of higher cumulative rainfall.

5. CONCLUSIONS

Based on our findings, hydrologically-based topographic assessments are very important to characterize EIL in response to hydrological conditions. Moreover, the assessment will be useful for considering topographic soil-water effect in EIL hazard assessments. For the next step, we will further investigate hydrological conditions of EIL in the field and correlate the field observations with GIS analysis to assess the direct evidence of the *degree of wetness* results.

REFERENCES

Bordoni, M., Meisina, C., Valentino, R., Lu, N., Bittelli, M., & Chersich, S. (2015). Hydrological factors affecting rainfall-induced shallow landslides: From the field monitoring to a simplified slope stability analysis. *Engineering Geology*, *193*, 19–37. https://doi.org/10.1016/j.enggeo.2015.04.006

Dahal, R. K., Hasegawa, S., Nonomura, A., Yamanaka, M., Masuda, T., & Nishino, K. (2009). Failure characteristics of rainfall-induced shallow landslides in granitic terrains of Shikoku Island of Japan. *Environmental Geology*, *56*(7), 1295–1310. https://doi.org/10.1007/s00254-008-1228-x

Koyanagi, K., Gomi, T., & Sidle, R. C. (2020). Characteristics of landslides in forests and grasslands triggered by the 2016 Kumamoto earthquake. *Earth Surface Processes and Landforms*, *45*(4), 893–904. https://doi.org/10.1002/esp.4781

Marc, O., Stumpf, A., Malet, J. P., Gosset, M., Uchida, T., & Chiang, S. H. (2018). Initial insights from a global database of rainfall-induced landslide inventories: The weak influence of slope and strong influence of total storm rainfall. *Earth Surface Dynamics*, *6*(4), 903–922. https://doi.org/10.5194/esurf-6-903-2018

Meunier, P., Hovius, N., & Haines, J. A. (2008). Topographic site effects and the location of earthquake induced landslides. *Earth and Planetary Science Letters*, *275*(3–4), 221–232.

Noviandi, R., Kharismalatri H. S., Gomi, T., Ishikawa, Y. (2019). Examining Landslide Materials Movement Using a Small Flume Experiment: A Case Study of the 2018 Eastern Iburi Earthquake , Hokkaido. *Japan Society of Erosion Control Engineering Meeting 2019, R4-025*

Ritonga, R. P., Gomi, T., Darma, S., Regan, T., Hefryan, K., Kharismalatri, S., Ishikawa, Y. (2021). Land Cover and Characteristics of Landslides Induced by the 2018 Mw 6.7 Eastern Iburi Earthquake , Hokkaido. *J-Stage*, *13*(3), 76–83.

Rózycka, M., Migoń, P., & Michniewicz, A. (2017). Topographic Wetness Index and Terrain Ruggedness Index in geomorphic characterisation of landslide terrains, on examples from the Sudetes, SW Poland. *Zeitschrift Fur Geomorphologie*, *61*(January), 61–80.

Saito, H., Uchiyama, S., Hayakawa, Y. S., & Obanawa, H. (2018). Landslides triggered by an earthquake and heavy rainfalls at Aso volcano, Japan, detected by UAS and SfM-MVS photogrammetry. *Progress in Earth and Planetary Science*, *5*(1), 1–10.

Sidle, R.C., Ochiai, H. (2006). Landslides: Processes, prediction, and land use. *Water Resources Monograph, American Geophysical Union*, Chapter 3, pp. 41-121.

Sidle, R. C., Greco, R., & Bogaard, T. (2019). Overview of landslide hydrology. *Water*, *11*(1), 11–13. https://doi.org/10.3390/w11010148

Tsuboyama, Y., Sidle, R. C., Noguchi, S., Murakami, S., & Shimizu, T. (2000). A zero-order basin - its contribution to catchment hydrology and internal hydrological processes. *Hydrological Processes*, *14*(3), 387–401.

Keyword: *Earthquake-induced landslide, topographic wetness index, landslide position*